

Transverse-mode selection in single-longitudinal-mode lasers

Oscar G. Calderón

Departamento de Óptica, Facultad de Ciencias Físicas, Universidad Complutense, Ciudad Universitaria s/n, 28040 Madrid, Spain

Víctor M. Pérez-García

Departamento de Matemáticas, Escuela Técnica Superior de Ingenieros Industriales, Universidad de Castilla-La Mancha, Campus Universitario s/n, 13071 Ciudad Real, Spain

I. Martín

Departamento de Informática y Automática, Facultad de Ciencias Físicas, Universidad Complutense, Ciudad Universitaria s/n, 28040 Madrid, Spain

J. M. Guerra

Departamento de Óptica, Facultad de Ciencias Físicas, Universidad Complutense, Ciudad Universitaria s/n, 28040 Madrid, Spain

(Received 19 July 1995)

In this paper we analyze the transverse pattern-forming characteristics of a two-level and single-longitudinal-mode laser. The corrections to the classical empty cavity modes due to pumping and losses are specifically considered, leading to different excitation rates for the different transverse modes. The near-threshold excitation rates provide a selection mechanism that is studied and compared to the results from numerical simulations of the Maxwell-Bloch equations.

PACS number(s): 42.60.Mi, 05.45.+b

I. INTRODUCTION

Lasers are among the most interesting devices found in optics, due to their dynamics, on which many studies have been based. In the last few years there has been an increasing interest in transverse effects in the context of pattern-formation problems [1], in both passive [2–6] and active systems [7–9]. The single-longitudinal-mode laser [8–10] has been a useful laboratory to study transverse phenomena without the influence of other degrees of freedom. For this reason a lot of work has centered around this mathematical model. The different approaches used to obtain information about the solutions of these equations include: exact solutions (nonlinear plane-wave models) [11], direct numerical simulations [12–17], reduction to simpler equations [14,18], discrete models [19], and especially empty cavity mode expansions [20–25]. The philosophy behind the latter approach is to expand the field inside the laser cavity on the basis of the empty cavity modes, which are known to have a clear physical relevance in many practical laser devices; i.e., the low Fresnel number systems tend to operate in a dynamical regime where few modes compete, one of which may sometimes be selected. In any case a few degrees of freedom are present in the dynamics usually corresponding to the laser modes [24,26,27]. With the words ‘‘laser mode’’ one usually refers to well-defined patterns having some similarities to the shape of the empty cavity modes. When a few of these modes are considered in the mathematical expansion one can find many different phenomena such as spontaneous symmetry breaking [28], cooperative frequency locking [29], chaotic itinerancy [30,31], chaotic alternation [32], etc. This approach has some important limitations. In the first place it is not possible to know *a priori* how many modes will be active in a particular system. This information is obtained later,

when some modes disappear and have no dynamical relevance. Another difficulty when using the empty cavity modes is that one is not sure whether the mode shape is more or less the same as that of the empty cavity modes, or the pumping and losses induce shape changes that affect the accuracy of the multimode expansion. Last, but not least, there is no way of knowing which, if any, will be the dominating mode in the dynamics without numerically integrating the set of coupled ordinary differential equations for the mode amplitudes.

In this paper, we try to address these questions by going a step beyond the usual empty cavity mode expansion, trying to see what the effect of losses and pumping is in a first approximation. The results are in a very good agreement with the numerical simulations of the partial differential equation and with physical experience [24].

II. STATEMENT OF THE GAIN-MODE PROBLEM

The starting point for our analysis is the Maxwell-Bloch equations for a polarized two-level laser with plane and parallel mirrors in the rotating wave, slowly varying amplitude, and single-longitudinal-mode approximations, which are [10]

$$\frac{\partial F}{\partial \tau} - \frac{i}{4\mathcal{L}} \Delta F + \sigma(F - P) = 0, \quad (1)$$

$$\frac{\partial P}{\partial \tau} + (1 + i\delta)P - FD = 0, \quad (2)$$

$$\frac{\partial D}{\partial \tau} + \gamma \left[D - r + \frac{1}{2}(F^*P + FP^*) \right] = 0, \quad (3)$$

where $\gamma = \gamma_{\parallel} / \gamma_{\perp}$ is the ratio between the depolarization time of the radiation-induced material dipoles (γ_{\perp}^{-1}) and the lifetime of the population inversion (γ_{\parallel}^{-1}). $\sigma = \sigma_c / (2\epsilon_0 \gamma_{\perp})$, σ_c measures the losses, including mirror coupling, internal transmission losses, aperture diffraction, etc. $\delta = (\omega_{12} - \omega_c) / \gamma_{\perp}$ is the rescaled detuning between the matter transition frequency and the fast oscillation of the field. $r = \alpha c / (\sigma \gamma_{\perp})$ is a rescaled pumping, i.e., $\alpha = \omega_{12} |\vec{D}_{12}|^2 N d_0 / (2\epsilon_0 \hbar \gamma_{\perp} c)$ is the small signal gain (\vec{D}_{12} being the dipole moment of the transition and N the number of atoms or molecules per unit volume in the active medium), and d_0 is the population inversion per atom or molecule induced by the pumping.

$\mathcal{F} = \pi b^2 / (\lambda L)$ is related to the Fresnel number ($\mathcal{F} = \pi F$), b is the transverse radius of the resonator, λ is the wavelength of the light, and L is the resonator length. The transverse rescaled variables are $\vec{\rho} = (\xi, \eta) = (x, y) / (b\sqrt{v})$, where $v = c / (L\gamma_{\perp})$, and the rescaled time variable is $\tau = \gamma_{\perp} t$.

Let us concentrate on the case where $|F|, |P| \ll 1$:

$$\begin{aligned} \frac{\partial F}{\partial \tau} - \frac{i}{4\mathcal{F}} \Delta F + \sigma(F - P) &= 0, \\ \frac{\partial P}{\partial \tau} + (1 + i\delta)P - FD &= 0, \end{aligned} \quad (4)$$

$$\Delta F + 4\mathcal{F} \left\{ \Omega + i\sigma - \frac{i\sigma r}{1 - i\Omega + i\delta} \frac{1}{1 + |F|^2 e^{i(\Omega^* - \Omega)\tau} [2 + i(\Omega^* - \Omega)] / 2(1 - i\Omega + i\delta)(1 + i\Omega^* - i\delta)} \right\} F = 0. \quad (7)$$

This is a nonlinear eigenvalue problem and a truly challenging mathematical problem. Let us then concentrate on the case where

$$|F|^2 \ll \frac{2(1 - i\Omega + i\delta)(1 + i\Omega^* - i\delta)}{2 + i(\Omega^* - \Omega)} e^{-i(\Omega^* - \Omega)\tau}. \quad (8)$$

Physically it corresponds to the first stages of the laser action, when the field is rising from zero in a small signal operation regime (near-threshold regime). Using (8) the following equation is found:

$$\Delta F + 4\mathcal{F} \left\{ \Omega + i\sigma - \frac{i\sigma r}{1 - i\Omega + i\delta} \right\} F = 0. \quad (9)$$

To close the mathematical problem we need to set up the reflecting type boundary conditions. This linear eigenvalue problem has only complex Ω solutions, which is why a complex Ω ($\Omega = \omega + i\kappa$) was considered from the beginning. The real part of Ω is related to the mode oscillation frequency while its imaginary part means the field initial slope, being positive if the field is amplified or negative if the field is damped. Then

$$\frac{\partial D}{\partial \tau} + \gamma(D - r) = 0.$$

Physically it corresponds to the first stages of the laser action, when the field is rising from zero in a small signal operation regime (near-threshold regime). The modes are solutions with a stationary spatial structure. Thus, let us consider during this first regime solutions with the particular time dependence

$$\begin{aligned} F(\tau, \vec{\rho}) &= F(\vec{\rho}) e^{-i\Omega\tau}, \\ P(\tau, \vec{\rho}) &= P(\vec{\rho}) e^{-i\Omega\tau}, \\ D &= D(\vec{\rho}), \end{aligned} \quad (5)$$

where Ω is related to the slow oscillation transverse-mode frequency. For reasons to be clarified later it will be considered a complex number. We assume the validity of the requirements,

$$|F(\vec{\rho}) e^{-i\Omega\tau}| \ll 1, \quad |P(\vec{\rho}) e^{-i\Omega\tau}| \ll 1, \quad (6)$$

and throughout the small-signal regime, we get the following equation for $F(\vec{\rho})$:

$$\begin{aligned} F(\tau, \vec{\rho}) &= F(\vec{\rho}) e^{-i\omega\tau} e^{\kappa\tau}, \\ P(\tau, \vec{\rho}) &= P(\vec{\rho}) e^{-i\omega\tau} e^{\kappa\tau}, \\ D &= D(\vec{\rho}). \end{aligned} \quad (10)$$

The physical reason for the need to complexify Ω is clear if we go back to Eqs. (1)–(3). Linearizing around $F = P = 0$, the resulting evolution equation is linear but non-conservative so that the solutions either explode or damp out to zero depending on whether the loss or gain term dominates (this can be easily checked by computing the evolution of the L^2 norm of the field, $I = \iint |F|^2 dx dy$). This being the case, the modes will either grow or decrease with time and this behavior is not included in a real Ω .

This treatment will strictly be applicable when the effects of the nonlinearities are negligible, corresponding to the approximation described in (8). The physical implications of the results to be presented here will be discussed later. Equation (9) now reads

$$\Delta F + 4\mathcal{F} \left\{ \omega + i\kappa + i\sigma - \frac{i\sigma r}{1 + \kappa - i(\omega - \delta)} \right\} F = 0. \quad (11)$$

The solutions of this problem in a sense contain more information than the linear modes, which are *static* objects and correspond to the limit of (11) where both the pumping and dissipation are set to zero. From now on, these will be referred to as gain modes or simply modes.

For the sake of simplicity we will consider a uniform pumping profile in the transverse direction, i.e., r constant. When using other pumping profiles, like the Gaussian profile, the thresholds and mode selection change (though probably not essential) and the TEM₀₀ structure is favored. This fact has been recently analyzed in [33].

III. GROWTH RATES, MODE SELECTION, AND NUMBER OF ACTIVE MODES

A. Calculation of the growth rates and oscillation frequencies of the modes

Since (11) is a linear equation, we can separate variables in polar coordinates

$$F(\vec{\rho}) = F(\rho, \theta) = F(\rho)H(\theta).$$

It is easily found that

$$H(\theta) = Ae^{im\theta} + Be^{-im\theta}, \quad m = 0, 1, 2, \dots \quad (12)$$

and

$$\rho^2 F'' + \rho F' + (a\rho^2 - m^2)F = 0 \quad \left(F' \equiv \frac{\partial F}{\partial \rho} \right), \quad (13)$$

where

$$a = 4\mathcal{F} \left\{ \omega + i\kappa + i\sigma - \frac{i\sigma r}{1 + \kappa - i(\omega - \delta)} \right\}.$$

Let us define the new (complex) variable $z = \rho\sqrt{a}$. The resulting equation is the well-known Bessel equation (with a complex variable)

$$z^2 \ddot{F} + z \dot{F} + (z^2 - m^2)F = 0 \quad \left(\dot{F} \equiv \frac{\partial F}{\partial z} \right). \quad (14)$$

The regular solutions of (12) are

$$F(z) = CJ_m(z).$$

Let us now impose the transverse boundary conditions, which will correspond to totally reflecting lateral surfaces at $x^2 + y^2 = b^2$ ($\rho = 1/\sqrt{v} \equiv \Theta$). In the real lasers, the electric field practically cancels out in the boundary region, because there used to be high losses (and additionally low pumping, if any) in the near boundary region. From a practical viewpoint this is practically equal to having high losses in the lateral surfaces. Then, our boundary condition (totally reflecting lateral surfaces) is in agreement with the electric field behavior. In the numerical simulations to be presented later we have also included a space-dependent loss function, with a sharp increase of the losses near the boundary.

The zero boundary condition implies that $J_m(\Theta\sqrt{a}) = 0$. But the zeros of this function are real numbers [34], in fact the real zeros of the Bessel functions (z_{mn}),

$$z_{mn} = \Theta\sqrt{a}.$$

Since a is a complex number ($a = a_1 + ia_2$) the last equation can also be written as

$$a_1 = \left(\frac{z_{mn}}{\Theta} \right)^2, \quad a_2 = 0. \quad (15)$$

The last two equations allow us to determine ω and κ :

$$\begin{aligned} \kappa + \sigma - \frac{\sigma r(1 + \kappa)}{(1 + \kappa)^2 + (\omega - \delta)^2} &= 0, \\ \omega + \frac{\sigma r(\omega - \delta)}{(1 + \kappa)^2 + (\omega - \delta)^2} &= \frac{1}{4\mathcal{F}} \left(\frac{z_{mn}}{\Theta} \right)^2. \end{aligned} \quad (16)$$

Let us define the new variables

$$\Gamma = \omega - \delta,$$

$$\Psi = 2\kappa + 1 + \sigma.$$

The new equation for Ψ is

$$\Psi^4 + [\beta_{mn}^2 - (1 - \sigma)^2 - 4\sigma r]\Psi^2 - (1 - \sigma)^2\beta_{mn}^2 = 0,$$

where $\beta_{mn} = (z_{mn}/\Theta)^2/(4\mathcal{F}) - \delta$. Solving this equation and rewriting the solution in terms of the old variables, we find the following expression for the solution:

$$\kappa = -\frac{1 + \sigma}{2} + \frac{1}{2} \sqrt{-\left(\frac{\beta_{mn}^2 - (1 - \sigma)^2 - 4\sigma r}{2} \right) + \sqrt{\left(\frac{\beta_{mn}^2 - (1 - \sigma)^2 - 4\sigma r}{2} \right)^2 + (1 - \sigma)^2\beta_{mn}^2}}. \quad (17)$$

The value of κ (15) can be used to calculate the oscillation frequency of each mode mn using the expression $\omega = \delta + (1 + \kappa)\beta_{mn}/(2\kappa + 1 + \sigma)$ and the result is

$$\omega = \delta + \left\{ 1 + \frac{1 - \sigma}{\sqrt{-\{[\beta_{mn}^2 - (1 - \sigma)^2 - 4\sigma r]/2\} + \sqrt{\{[\beta_{mn}^2 - (1 - \sigma)^2 - 4\sigma r]/2\}^2 + (1 - \sigma)^2\beta_{mn}^2}}} \right\} \frac{\beta_{mn}}{2}. \quad (18)$$

It is then seen that the mode frequencies depend on both σ and r , so that our approach provides additional information to that given by the empty cavity theory, where the mode oscillation frequencies depend only on the geometrical characteristics of the resonator and are not influenced by the parameters. The angular frequency is, of course, in units of γ_{\perp} .

B. Selection of amplified modes

Since the function κ (17) contains the information on how the different spatial structures grow, it is interesting to analyze it in more detail. In the first place, it is possible to find which mn mode has the largest κ . The maximum growth rate is given by

$$\frac{d\kappa}{d\beta_{mn}} = \frac{1}{2\sqrt{2A}}\beta_{mn} \left[-1 + \frac{\beta_{mn}^2 + (1-\sigma)^2 - 4\sigma r}{\sqrt{(\beta_{mn}^2 + (1-\sigma)^2 - 4\sigma r)^2 + 16(1-\sigma)^2\sigma r}} \right] = 0, \quad (19)$$

where

$$A = -\left(\frac{\beta_{mn}^2 - (1-\sigma)^2 - 4\sigma r}{2}\right) + \sqrt{\left(\frac{\beta_{mn}^2 - (1-\sigma)^2 - 4\sigma r}{2}\right)^2 + (1-\sigma)^2\beta_{mn}^2}.$$

It is easy to see that the maximum corresponds to $\beta_{mn} = 0$. Thus the mode (if any) whose zero satisfies

$$\delta = \frac{1}{4\mathcal{F}} \left(\frac{z_{mn}}{\Theta}\right)^2 \quad (\beta_{mn} = 0) \quad (20)$$

will have an amplitude with the fastest amplitude increase, and its oscillation frequency and rate of increase will be equal to

$$\omega = \delta, \quad (21)$$

$$\kappa = -\frac{1+\sigma}{2} + \sqrt{\left(\frac{1-\sigma}{2}\right)^2 + \sigma r}.$$

When none of the zeros z_{mn} satisfies exactly (18), but there is one mode satisfying $(z_{mn}/\Theta)^2/(4\mathcal{F}) - \delta = \epsilon$ with small ϵ , it is found that

$$\omega \simeq \delta + \frac{\epsilon}{2} \left[1 + \frac{1-\sigma}{\sqrt{(1-\sigma)^2 + 4\sigma r}} \right], \quad (22)$$

$$\kappa \simeq -\frac{1+\sigma}{2} + \sqrt{\left(\frac{1-\sigma}{2}\right)^2 + \sigma r}.$$

With this information for a given set of physical parameters we are able to determine which is the fastest growing mode, and what the growing rates of the other ones are. The modes with a positive κ value grow exponentially, while the modes whose κ value is negative decrease. The decreasing modes are not expected to contribute to the final asymptotic state, so that determining the κ sign of a mode, the relevant modes can be predicted *a priori*. When only one mode has a positive κ value, it will probably be selected. After an initial regime described by (9), the electric field will contain mostly this spatial mode. The parameters can be set up so that only one mode is amplified, which means that Eq. (17) can be very useful from the viewpoint of applications, where sometimes only one specific mode is desired.

It is also possible that several modes grow ($\kappa > 0$). In this case the situation is more complicated because after the first stages, all these modes can take part in the field dynamics.

Let us analyze in more detail the shape of $\kappa(\beta_{mn})$ in order to find what modes are amplified.

In the limit of high z_{mn} values (high-order modes) we find

$$\lim_{\beta_{mn} \rightarrow \infty} \kappa_{mn} = \begin{cases} -\sigma & \text{if } \sigma < 1 \\ -1 & \text{if } \sigma \geq 1, \end{cases} \quad (23)$$

so that very high order modes are damped. The zeros of $\kappa(\beta_{mn})$ determine which modes are the last to be amplified:

$$\beta_{mn}^2 = (1+\sigma)^2(r-1).$$

Thus, if $\beta_{mn}^2 < \widetilde{\beta}^2$ the modes grow and they decrease exponentially if the contrary is the case. The condition for a mode to be amplified is then that

$$\beta_{mn}^2 < (1+\sigma)^2(r-1).$$

If $r < 1$, the inequality cannot be satisfied and all the modes decrease. In the contrary case the modes grow. This has been checked in the numerical calculations and means that the threshold for the laser action is $r = 1$. Assuming then that $r > 1$,

$$\left| \frac{1}{4\mathcal{F}} \left(\frac{z_{mn}}{\Theta}\right)^2 - \delta \right| < (1+\sigma)\sqrt{r-1}. \quad (24)$$

In general, this equation states that the modes whose zeros (z_{mn}) satisfy the inequality are amplified (with different rates

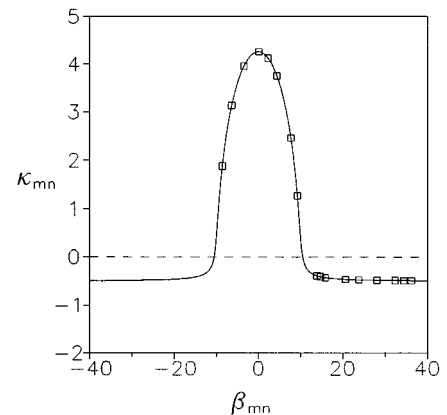


FIG. 1. Growth rates of the different modes for parameter values: $r=50$, $\sigma=0.5$, $\mathcal{F}=1$, $\Theta=1.0$, and $\delta=10.0$.

as described above) and their participation in the asymptotic dynamics can be important. Figure 1 shows the growth rates for a particular set of parameter values. The modes under the dashed line are damped. In this case, there are only eight active modes.

If there is one mode, its zero satisfying Eq. (20), then this mode is the one with the highest growth rate. Let us then denote it by z_{opt} . The inequality (24) can be rewritten as

$$|z_{mn}^2 - z_{\text{opt}}^2| < 4\mathcal{F}\Theta^2(\sigma+1)\sqrt{r-1}. \quad (25)$$

C. Number of active modes

By applying the more general expression (24) we can estimate the number of modes that can oscillate in the resonator. If δ is smaller than $(z_{00}/\Theta)^2/(4\mathcal{F})$, β_{mn} is always positive. Taking away the absolute value we find

$$z_{mn} < \Theta \sqrt{4\mathcal{F}[(1+\sigma)\sqrt{r-1} + \delta]}. \quad (26)$$

Since $z_{0n} \approx \pi(n+3/4)$, $n=0,1,2,\dots$ the maximum value of n that complies with the inequality is

$$n_{\text{max}} = \frac{\Theta}{\pi} \sqrt{4\mathcal{F}[(1+\sigma)\sqrt{r-1} + \delta]} - \frac{3}{4}$$

and the number of modes with $m=0$ that can oscillate is $n_{\text{max}} + 1$. Considering how the zeros values (z_{mn}) are distributed in the different modes (mn), the total number of radial structures oscillating in the resonator (N_{rad}) is

$$N_{\text{rad}} = (n_{\text{max}} + 1) + \sum_{j=1}^{n_{\text{max}}} 2[(n_{\text{max}} + 1) - j] = (n_{\text{max}} + 1)^2.$$

Since we have two angular structures corresponding to the same value of m the total number of modes is

$$N_{\text{modes}} = 2N_{\text{rad}} - 1 \approx \left(\frac{\Theta}{\pi}\right)^2 8\mathcal{F}[(1+\sigma)\sqrt{r-1} + \delta].$$

For instance, when r is large the number of active modes can be very large, even when the Fresnel number is small. In the limit of large r values, the number of modes is given by

$$N_{\text{modes}} \approx \left(\frac{\Theta}{\pi}\right)^2 8\mathcal{F}\sqrt{r}(1+\sigma). \quad (27)$$

The number of modes that are amplified in the resonator is proportional to the Fresnel number. It must be said that these are the amplified modes and that this restriction has nothing to do with the usual limit to the number of modes that can oscillate in a passive cavity, which is related to the geometrical considerations [35]. In particular, in the case of a passive system the Fresnel number dependence is on \mathcal{F}^2 while in our active system we have found a linear dependence on \mathcal{F} . A similar dependence (linear on \mathcal{F}) has been found in [3] for a photorefractive oscillator.

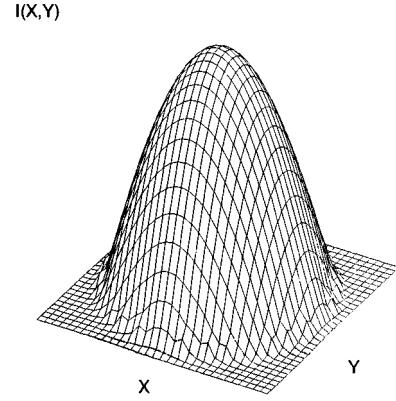


FIG. 2. Stationary pattern found for $r=12.4$, $\gamma=0.1$, $\sigma=0.1$, $\delta=5.78$, $\mathcal{F}=1$, and $\Theta=0.5$.

D. Maximum transverse mode beating frequency

The maximum frequency that can be generated by transverse mode beating is provided by the difference between the more distant amplified modes in the transverse spectrum, i.e.,

$$\begin{aligned} \Delta\omega &= \omega[\beta_{mn} = (1+\sigma)\sqrt{r-1}] \\ &\quad - \omega[\beta_{mn} = -(1+\sigma)\sqrt{r-1}] \\ &= 2\sqrt{r-1}. \end{aligned}$$

IV. NUMERICAL RESULTS

In the previous sections we have obtained a series of formulas for the modes that are excited in the cavity during the initial regime. To what extent will the results hold when the nonlinearities govern the dynamics? Since analytical treatment of the nonlinear eigenvalue problem is not possible, the only way to answer this question is to make numerical simulations and to compare the results with the predictions for the low signal regime. Our guess is that once the nonlinear state is reached the modes initially excited will remain the active laser modes and that the effect of the nonlinearity will be mainly reduced to mix the amplitudes and induce multimode oscillations, etc. In principle, it is also possible that the most active mode is the only one surviving in the stationary state.

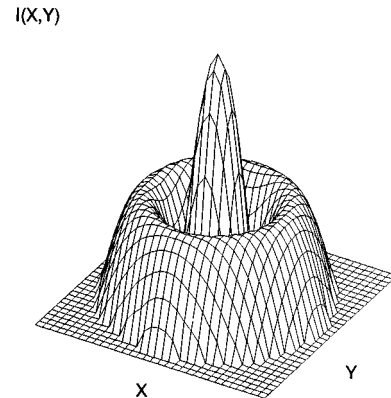


FIG. 3. Stationary pattern found for $r=60.0$, $\gamma=0.1$, $\sigma=0.1$, $\delta=7.61$, $\mathcal{F}=4$, and $\Theta=0.5$.

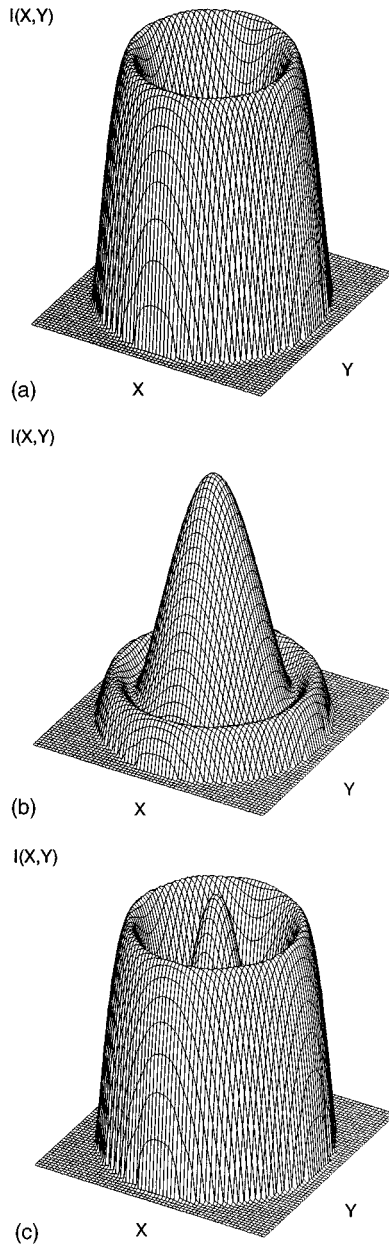


FIG. 4. Different spatial profiles found for $r=15.0$, $\gamma=0.1$, $\sigma=0.1$, $\delta=3.65$, $\mathcal{F}=4$, and $\Theta=0.5$. (a) $\tau=3.0$, (b) $\tau=7.0$, (c) $\tau=14.0$.

This could occur when the gain of one mode is much higher than the gain of the rest of the modes.

To check these conjectures we have numerically integrated the single-longitudinal-mode Maxwell-Bloch equations using a very efficient full multigrid implementation of a linear finite-difference scheme [13,17,36]. The gain profile was flat inside the integration region and the losses are suddenly increased from zero to a very high value in the boundary region so that an effective limitation to the solution to the region of interest is obtained. The initial condition for the field was either flat or Gaussian with radial symmetry.

Generally speaking in the initial regime, where the analytical treatment is accurate, the numerical solutions resemble the predicted behavior, the most excited mode being the one predicted theoretically as should be expected from

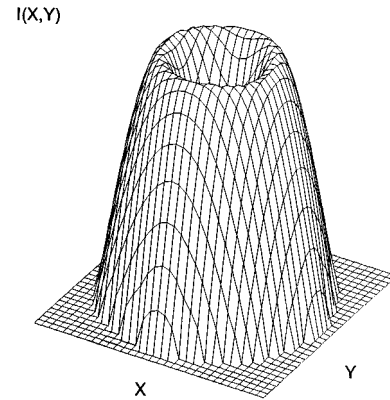


FIG. 5. Stationary state for parameter values: $r=3$, $\gamma=0.1$, $\sigma=0.1$, $\delta=3.67$, $\mathcal{F}=4$, and $\Theta=0.5$.

the good behavior of the numerical scheme.

We will now focus our interest on the long-term asymptotic solution, where the nonlinearities can be important.

First of all the equations with parameters $r=12.4$, $\gamma=0.1$, $\sigma=0.1$, $\delta=5.78$, $\mathcal{F}=1$, and $\Theta=0.5$ have been integrated. In this situation Eq. (15) predicts that the $m=0$, $n=0$ mode is much more amplified than the other ones. The numerical result for the stationary profile is shown in Fig. 2, this being clearly a 00 structure.

Second, we have integrated the equations with parameters $r=60.0$, $\gamma=0.1$, $\sigma=0.1$, $\delta=7.61$, $\mathcal{F}=4$, and $\Theta=0.5$. The theoretical prediction is that the $m=0$, $n=1$ mode, having a zero at a given radial distance before the one on the border and radial symmetry, is the most amplified one. The numerical result for the stationary pattern is shown in Fig. 3 and is in agreement with our prediction. We have checked that this behavior is not exclusive for this parameter combination but is also predicted and found for $r=45$, $r=20$, and $r=2$.

Finally, when the parameters are set to $r=15.0$, $\gamma=0.1$, $\sigma=0.1$, $\delta=3.65$, $\mathcal{F}=4$, and $\Theta=0.5$, we predict that the most excited mode is the one with $m=1$ and $n=0$ (which has a zero at the origin) and other modes have near excitation rates. The numerical result shows that during the initial stage this mode is selected [Fig. 4(a)] but then others such as the 00 appear, initiating a competition with some intermediate steps [Figs. 4(b) and 4(c)] and ultimately behaving periodically with time (multimode oscillation regime).

In this case we also checked a parameter combination where the only mode with a positive growth rate is the one with $m=1$, $n=0$ ($r=3$, $\gamma=0.1$, $\sigma=0.1$, $\delta=3.67$, $\mathcal{F}=4$, and $\Theta=0.5$). In the asymptotic state only this mode appears (Fig. 5) and there are no tracks of mode competition.

All this evidence indicates that the theoretical predictions are good, not only in the initial regime where the approximations are valid, but also in the stationary behavior.

V. CONCLUSIONS

In this study we have extended the much used empty cavity theory to include in a first approximation the effect of the losses and the pumping, which are present in the laser system, so that not only geometrical considerations are made.

Our model allows us to predict what modes will increase, what their growth rates and oscillation frequencies will be, and how many modes are expected to coexist in the multimode regimes. In the latter case a linear dependence in the Fresnel number is predicted, which is caused by the selection mechanism different from purely geometrical considerations.

It must be said that our approach is not expected to be applicable beyond the low Fresnel number (and low gain) regions, which is where multimode expansions make sense [19,24,37].

Some of the predictions of our model have been com-

pared with numerical simulation results and a very good agreement is found.

We are preparing an experiment with a single longitudinal CO₂ laser, which will be a real test bed for our theoretical and numerical predictions.

ACKNOWLEDGMENTS

This work has been partially supported by the ‘‘Plan General de Promoción del Conocimiento’’ under Project No. PB92-0798.

-
- [1] M.C. Cross and P.C. Hohenberg, *Rev. Mod. Phys.* **65**, 851 (1993).
- [2] F.T. Arecchi, G. Giacomelli, P.L. Ramaza, and S. Residori, *Phys. Rev. Lett.* **65**, 2531 (1990); **67**, 3749 (1990); E. Pampaloni, S. Residori, and F.T. Arecchi, *Europhys. Lett.* **24**, 647 (1993).
- [3] F.T. Arecchi, S. Boccaletti, P.L. Ramaza, and S. Residori, *Phys. Rev. Lett.* **70**, 2277 (1993).
- [4] M. Brambilla, G. Broggi, and F. Prati, *Physica D* **58**, 339 (1992).
- [5] G.L. Oppo, M. Brambilla, and L.A. Lugiato, *Phys. Rev. A* **49**, 2028 (1994).
- [6] M.A. Vorontsov and W.J. Firth, *Phys. Rev. A* **49**, 2891 (1994).
- [7] L.A. Lugiato, W. Kaige, and N.B. Abraham, *Phys. Rev. A* **49**, 2049 (1994).
- [8] P.K. Jakobsen, J.V. Moloney, A.C. Newell, and R. Indik, *Phys. Rev. A* **45**, 8129 (1992).
- [9] P.K. Jakobsen, J. Lega, Q. Feng, M. Stanley, J.V. Moloney, and A.C. Newell, *Phys. Rev. A* **49**, 4189 (1994).
- [10] L.A. Lugiato, G.L. Oppo, J.R. Tredicce, L.M. Narducci, and M.A. Pernigo, *J. Opt. Soc. Am. B* **7**, 1019 (1990).
- [11] I. Pastor, V.M. Pérez-García, F. Encinas-Sanz, J.M. Guerra, and L. Vázquez, *Physica D* **66**, 421 (1993).
- [12] R. Indik and A.C. Newell, *Math. Comp. Simul.* **37**, 385 (1994).
- [13] I. Martín, V.M. Pérez-García, J.M. Guerra, F. Tirado, and L. Vázquez, *Fluctuation Phenomena: Disorder and Nonlinearity*, edited by A.R. Bishop, S. Jiménez, and L. Vázquez (World Scientific, Singapore, 1995).
- [14] K. Staliunas, *Phys. Rev. A* **49**, 1573 (1993).
- [15] P. Couillet, L. Gil, and F. Rocca, *Opt. Commun.* **73**, 403 (1989).
- [16] E. D’ Angelo, C. Green, J.R. Tredicce, N.B. Abraham, S. Balle, Z. Chen, and G.L. Oppo, *Physica D* **61**, 6 (1992).
- [17] B.Y. Guo, I. Martín, V.M. Pérez-García, and L. Vázquez (unpublished).
- [18] J. Lega, P.K. Jakobsen, J.V. Moloney, and A.C. Newell, *Phys. Rev. A* **49**, 4201 (1994).
- [19] V.M. Pérez-García and J.M. Guerra, *Phys. Rev. A* **50**, 1646 (1994).
- [20] M. Brambilla, F. Battipede, L.A. Lugiato, V. Penna, F. Prati, C. Tamm, and C.O. Weiss, *Phys. Rev. A* **43**, 5090 (1991).
- [21] M. Brambilla, L.A. Lugiato, V. Penna, F. Prati, C. Tamm, and C.O. Weiss, *Phys. Rev. A* **43**, 5155 (1991).
- [22] W. Kaige, N.B. Abraham, and L.A. Lugiato, *Phys. Rev. A* **47**, 1263 (1994).
- [23] M. Brambilla, M. Cataneo, L.A. Lugiato, R. Pirovano, F. Prati, A.J. Kent, G.L. Oppo, A.B. Coates, C.O. Weiss, C. Green, E.J. D’ Angelo, and J.R. Tredicce, *Phys. Rev. A* **49**, 1427 (1994).
- [24] A.B. Coates, C.O. Weiss, C. Green, E.J. D’ Angelo, J.R. Tredicce, M. Brambilla, M. Cataneo, L.A. Lugiato, R. Pirovano, F. Prati, A.J. Kent, and G.L. Oppo, *Phys. Rev. A* **49**, 1452 (1994).
- [25] F. Prati, M. Brambilla, and L.A. Lugiato, *Riv. Nuovo Cimento* **17**, 1 (1994).
- [26] I. Pastor, F. Encinas, and J.M. Guerra, *Appl. Phys. B* **52**, 184 (1991).
- [27] J.M. Guerra, F. Encinas, and I. Pastor, in *Third International Workshop on Nonlinear Dynamics and Quantum Phenomena in Optical Systems*, Springer Proceedings in Physics Vol. 55, edited by R. Vilaseca and R. Corbalán (Springer-Verlag, Berlin, 1991).
- [28] L.A. Lugiato, F. Prati, L.M. Narducci, and G.L. Oppo, *Opt. Commun.* **69**, 387 (1989).
- [29] L.A. Lugiato, G.L. Oppo, M.A. Pernigo, J.R. Tredicce, and L.M. Narducci, *Opt. Commun.* **68**, 63 (1988).
- [30] K. Ikeda, K. Otsuka, and K. Matsumoto, *Prog. Theor. Phys. Suppl.* **99**, 295 (1989).
- [31] K. Otsuka, *Phys. Rev. Lett.* **65**, 329 (1990).
- [32] F.T. Arecchi, S. Boccaletti, G.B. Mindlin, and C. Pérez García, *Phys. Rev. Lett.* **69**, 3723 (1992).
- [33] G.H. Harkness and W.J. Firth, *J. Mod. Opt.* **39**, 2023 (1992).
- [34] G.N. Watson, *A Treatise on the Theory of Bessel Functions* (Macmillan, New York, 1948).
- [35] A. Siegman, *Lasers* (Oxford University Press, New York, 1985).
- [36] I. Martín, Ph.D. thesis, Universidad Complutense, Madrid, 1995 (unpublished).
- [37] V.M. Pérez-García, I. Pastor, and J.M. Guerra, *Phys. Rev. A* **52**, 2392 (1995).